DOI: 10.1007/s12541-012-0192-2

A Robotic Colonoscope with Long Stroke and Reliable Leg Clamping

Hyun-jun Park[1], Dowon Kim[1], and Byungkyu Kim[1,#]

1 School of Aerospace and Mechanical Engineering, Korea Aerospace University, Hwajeon-dong, Deogyang-gu, Goyang-si, Gyeonggi-do, Korea, 412-791
Corresponding Author / E-mail: bkim@kau.ac.kr, TEL: +82-2-300-0101, FAX: +82-2-3158-5769

KEYWORDS: Inchworm-like mechanism, Colonoscope, Robot, Pneumatic

Previously developed robotic colonoscopes have shown low locomotion performance since they have not had reliable clamping modules or a long stroke. Therefore, a clamping module consisting of six legs and two triggers is installed on the front and rear of the robot, enabling the robot to clamp effectively onto the colon. Locomotion capability is then improved via the on-time folding and unfolding of the legs according to the elongation and contraction of the bellows of the robot body. In addition, one pneumatic line based locomotive mechanism, which had been developed previously for in-pipe inspection, is adopted to reduce the friction force between the pneumatic lines and the locomotion environment. In order to evaluate locomotion performance, the robot and robot control system are constructed and are tested in an acrylic pipe and under condition of in-vitro. The robot can move regardless of slope in the case that the locomotion path has more than 25 mm of radius. In straight and vertical paths, it travels 33 mm/s and 12.1 mm/s, respectively. Next, a locomotion test under in-vivo condition is carried out with the optimized configuration and maneuvering parameters. Conclusively, a pneumatic bellows based locomotive mechanism with a dependable clamping module shows the reliable locomotion performance of about 8.5 mm/sec under in-vivo condition.

Manuscript received: July 12, 2011 / Accepted: February 2, 2012

1. Introduction

Since 2000, we have been developing robotic colonoscopes based on a link mechanism,[1] radial wheel,[2] a pneumatic impulsive device,[3] a tendon-driven clamping mechanism,[4] a paddling-like mechanism,[5] and an inchworm-like mechanism.[6] There has also been a lot of effort to develop robotic colonoscopies by using a flexible chain,[7,8] a clamping segment with inflatable balloons,[9] a robotic legged capsule,[10] a snake-like mechanism[11] and a parallel manipulator-integrated endoscope.[12] In addition, in-vitro and in-vivo tests have been performed in other institutes.[13-15] In particular, inchworm-like locomotion has been popularly employed as a bio-mimetic approach. It has been shown that inchworm-type devices have the capability to overcome the flexibility and the slipperiness of a colon. Usually, they utilize flexible bellows for elongation and contraction, and suction based clampers for clamping and releasing. Therefore, at least three pneumatic lines are required to supply the air for each chamber: the front clamper, the bellows and the rear clamper.[13,16] For perfect clamping, some extra time is required, and a red mark remains. That can lead to an erroneous diagnosis. In order to reduce red marks and the loss of locomotion capability due to extra suction and insufflation, the suction based clampers are replaced by legs based clampers in this article. In addition, a previously developed one pneumatic line based inchworm-like mechanism for in-pipe inspection is adopted to reduce the friction force between the pneumatic lines and the locomotion environment.[17] To find optimized operation parameters, the velocity under variation of suction and blowing time is investigated with a theoretical approach. Then, experiments under in-vitro and in-vivo condition are carried out with some optimized parameters.

2. Robot system

2.1 Robot structure

As in Fig. 1, the robot consists of two main modules: the bellows and two clampers (front and rear). As previously mentioned, realizing perfect clamping on a slippery colon is far from easy; this is the main obstacle to overcome in the development of a reliable robotic colonoscope. For our proposed robotic colonoscope, we employ a six-leg based clamper that can be folded and unfolded

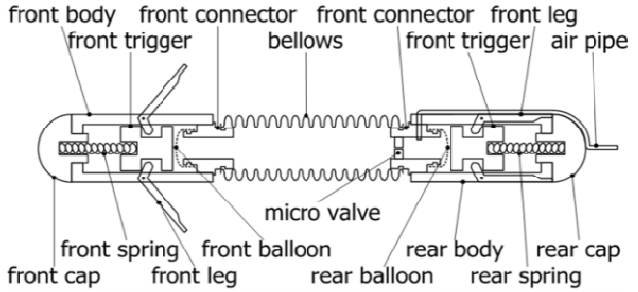

Fig. 1 Schematic of inchworm-like robotic colonoscope

according to the position of a trigger. The position of each trigger installed in the front and rear clampers is decided according to the expansion and contraction of a balloon since the trigger mechanism is activated using the interaction between pressure in the bellows and the springs in the front and rear clampers. As a kind of counter spring for the balloon, therefore, each spring in the front and rear clampers is installed. They play a role in returning the trigger to its initial position. In order to achieve long stroke per on-time insufflation and suction, a bellows is employed. In particular, a micro valve is allocated between the rear clamper and bellows to compensate the flow rate difference between the air compressor and suction device.

2.2 The working principle

Fig. 2 shows the sequence for the forward movement of the robotic colonoscope. (0) As its initial state, the bellows is under a neutral condition of atmospheric pressure, and the front and rear legs are unfolded and folded, respectively. (1) As the air is pumped out using a suction device, the bellows is contracted. The front and rear legs keep unfolding and folding, respectively. (2) After the suction is stopped, the pneumatic line switches to a compressor and the air is insufflated in the bellows. Next, the bellows is expanded and the front and rear balloons are also expanded to the front and rear sides, respectively. (3) This results in the pushing of each trigger. Consequently, the front legs are folded and the rear legs are unfolded. (4) After the robot body fully expands, the insufflation is stopped and the line connection is switched to the suction device. Then, the balloons are contracted, and the front and rear springs return the triggers to their initial position. This makes the front legs unfold and the rear legs fold. (5) As the suction device pumps out the air, the bellows contracts and a stroke is achieved.

2.3 System configuration

The designed robotic colonoscope is represented in Fig. 3. For the main body of the robot, the bellows is made of polyethylene. It has a peak diameter of 15 mm, a valley diameter of 9 mm, a pitch of 2 mm and a body thickness of 0.5 mm. Considering biocompatibility, the leg is made of stainless steel. Also, the other components, such as the robot body, cap, trigger, micro valve and connection pieces, are made of PEEK, which is a biocompatible material. Both the front and rear bodies are 30 mm in length, and the bellows is 100 mm in length under atmospheric pressure. According to the amount of pressure being applied, the contracted and expanded lengths of the robot are 110 mm and 250 mm, respectively. The maximum diameter of the

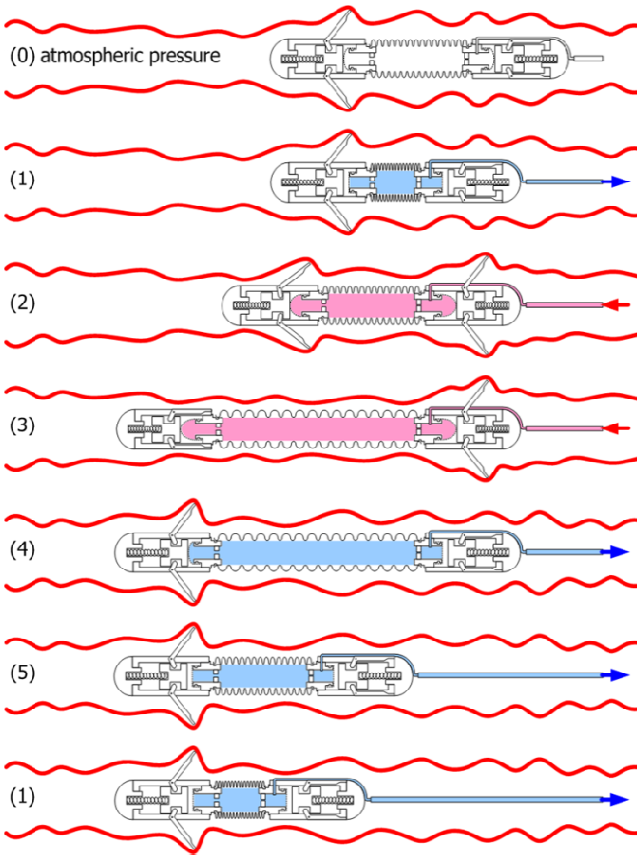

Fig. 2 Locomotive principle of robotic colonoscope

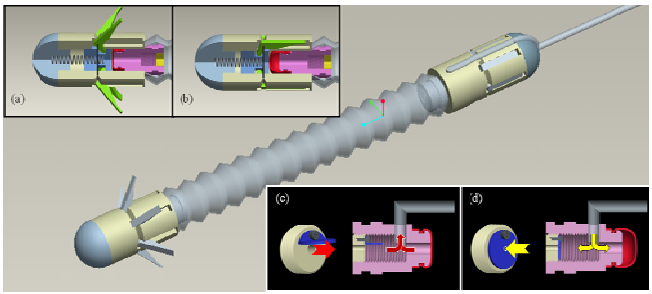

Fig. 3 Robot design (a) in the case of suction, legs are unfolded (b) in the case of blowing, legs are folded (c) in the case of suction, the microvalve is opened and the air passes through the big hole (d) in the case of blowing, the microvalve is closed and the air passes through the small hole

robot is 15 mm. The total mass of the robot is 16.5 g. The compressor and suction generator with high capacity are beneficial for increasing the velocity of the robot. Usually, however, the capacity of a compressor is higher than that of a suction generator. Therefore, more suction time is required than insufflation time. This causes a reduction in robot velocity. Therefore, a micro valve as shown in Fig. 3(c) and (d) is installed to control the flow rate properly. When the air insufflates, the air passes through a small-sized hole (e.g. 0.1 mm). For suction of the air, the air passes through a large-sized hole (e.g. 1 mm). In Fig. 4, the fabricated robot and the robot control system are presented. A compressor and a vacuum generator are employed to control the pneumatic pressure in the robot body. To control the electrical signal, LabVIEW®8.5 is utilized. Based on

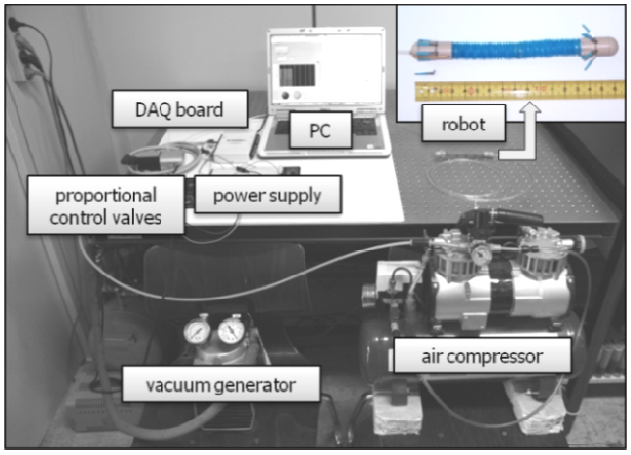

Fig. 4 Robot system configuration

Table 1 Specification of pressure control system

Air compressor	650 kPa
Vacuum generator	17.33 kPa
Control program	NI LabVIEW 8.5
DAQ board	NI USB 6218
Proportional control valves	FESTO MPPE-3-1/8-10-010B
Power supply	24V, 0.6A

the signal from LabVIEW, the magnitude of the pressure, blowing and suction time is controlled by the pneumatic valve (FESTO®). The specifications of the pressure control system are summarized in Table 1.

3. Theoretical and experimental results

3.1 Theoretical analysis

As previously mentioned in Section 2.2 and 2.3, the speed of the robot is determined according to control parameters such as the air pressure, suction and blowing time, and the hole size of the micro valve between the bellows and the rear body. Therefore, we investigate the main parameters that influence the velocity of the robot theoretically by developing a code for simulation. In order to simplify the simulation, theoretical analysis is carried out only for the bellows. This is done with certain assumptions taken into account; namely, no bellows expansion to the radial direction, no change of hole size between bellows and rear chamber, and no change of bellows characteristics under repeated experiments.

The theoretical analysis procedure is proposed as follows.

1) The control volume form of the first law of thermodynamics is as follows;

$$e = u + \frac{V^2}{2} + gz \tag{1}$$

Here, we assume $\dot{W} \approx 0$ and the flow is steady and incompressible. The internal energy and pressure at section ① and ② in Fig. 5 are uniform.

2) Then we can obtain the energy equation in the pipe flow.

$$\left(\frac{P_1}{\rho} + \alpha_1 \frac{\bar{v}_1^{\,2}}{2} + gz_1\right) - \left(\frac{P_2}{\rho} + \alpha_2 \frac{\bar{v}_2^{\,2}}{2} + gz_2\right) = H_{l_T} \tag{2}$$

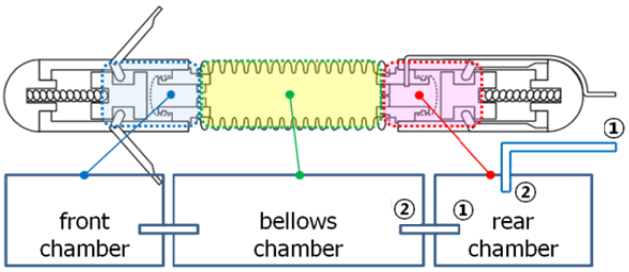

Fig. 5 Schematic diagram of robot for simulation

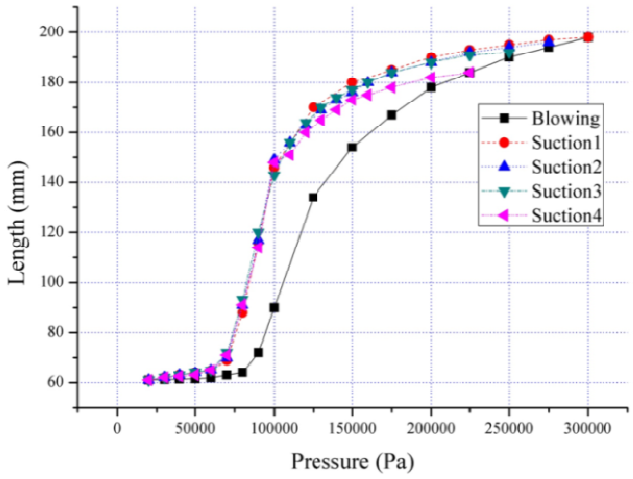

Fig. 6 Experimental data for length of bellows according to inner pressure of bellows

3) If we assume $\alpha_1, \alpha_2 \approx 1$, $z_1 \approx z_2$ and $\bar{v}_1 \approx 0$, equation (2) can be arranged for $\bar{v}_2$ of air flow velocity to the bellows as equation (3).

$$\bar{v}_2 = 1.414\sqrt{P_1 - P_2 - H_{l_T}}/\sqrt{\rho} \tag{3}$$

4) The mass flow rate to the bellows is calculated by employing equation (4).

$$\dot{m} = \rho A \bar{v}_2 = 1.414 A \sqrt{P_1 - P_2 - H_{l_T}}\sqrt{\rho} \tag{4}$$

A: Cross section area of the tube between the two chambers
H_{lT}: Energy loss due to pipe flow
P_1, P_2: Pressure at each section ① and ②
ρ: Density of the air

5) Next, the total mass of the air in the bellows is obtained with equation (5). The current total mass is calculated by adding the previous mass and increment mass, which is obtained by multiplying the time step and the mass flow rate as follows;

$$m_2 = m_{2,i} + \dot{m}\Delta t \tag{5}$$

6) Finally, the pressure and volume of the bellows are simultaneously calculated using the ideal gas equation (6) and a function (volume versus pressure) obtained from the experimental data in Fig. 6.

$$PV = mRT \tag{6}$$

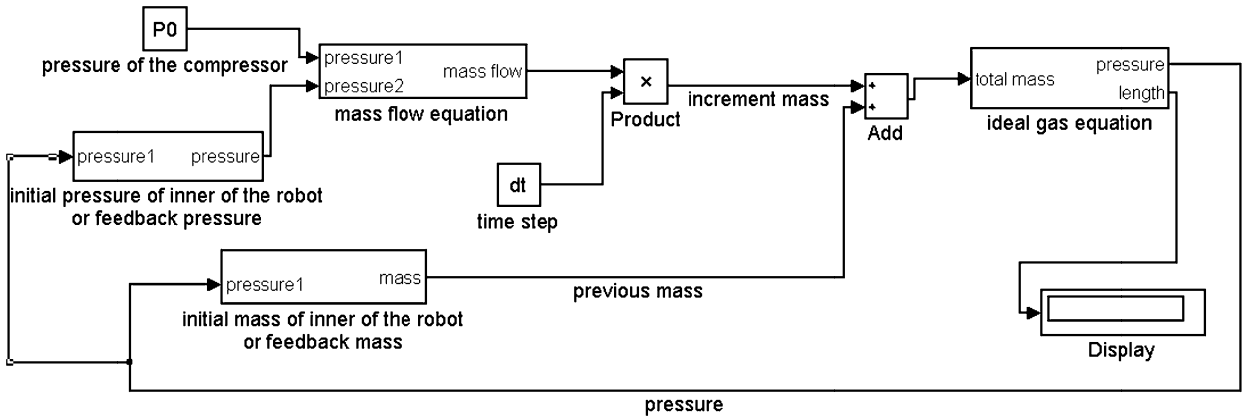

Fig. 7 Simulation flow chart for robot locomotion

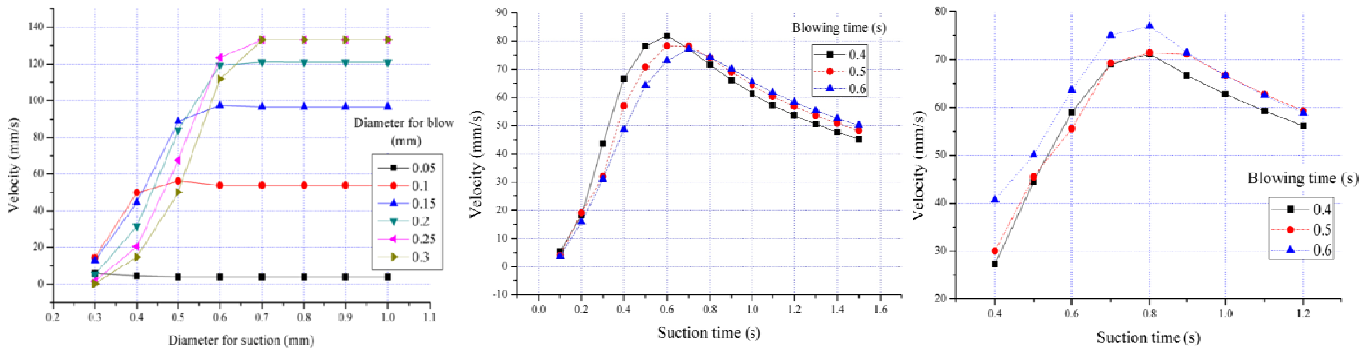

(a) (b) (c)

Fig. 8 (a) Theoretical velocity according to the size of the hole between rear chamber and bellows (b) theoretical velocity according to changed blowing and suction time (c) experimental velocity according to changed suction and blowing time

Where, V is volume, m is mass, P is pressure, T is temperature and R is gas constant.

7) By iteration of processes (3)~(6) with the new calculated pressure, the length of the bellows according to pressure can be obtained during the whole suction and blowing procedure. Accordingly, the length as a function of time, that is velocity, can be represented using a time step based volume presentation. As we can expect from these equations, the main parameters for the velocity of the robot are hole sizes *A* between the chambers, and air suction and blowing time. Therefore, the velocity of the robot according to changes of hole sizes and suction and blowing time is calculated using the flow chart in Fig. 7. For simulation, the range of hole sizes in the cases of blowing and suction is employed as 0.1~1.0 mm. Here, the inlet and outlet pressure is 650 kPa and 17.33 kPa, respectively. The simulation results in Fig. 8(a) show that the hole for insufflation should be in the range of 0.1~0.25 mm, and the hole for suction should be bigger than 0.7 mm. Based on these simulation results, the robot is fabricated with a hole of 0.1 mm for blowing and a hole of 1 mm for suction. In order to investigate the optimized control parameters for the fabricated robot, the velocity of the robot is evaluated under a variation of suction and blowing times in Fig. 8(b).

3.2 Experimental results

3.2.1 Functional test

With the optimized suction and blowing times investigated in Fig. 8(b), and the fixed blowing pressure of 650 kPa, and the suction pressure of 17.33 kPa, the functional tests are carried out. The velocity is then calculated using a video clip capturing the motion of the robot in a 20 mm diameter acrylic pipe. When the suction time is less than 0.8 sec, however, enough stroke is not generated. This causes a reduction in velocity. When it is higher than 0.8 sec, there is no more shrinkage after 0.8 sec, and the robot is under idling condition. As shown in Fig. 8(c), therefore, the robot velocity is highest when suction time is around 0.8 sec. On the other hand, the blowing time does not significantly influence the velocity of the robot since the rate of expansion increase, according to the increase of pressure, decreases after the bellows increases beyond the linear relation between bellows length and pressure (Fig. 6). Consequently, the most promising velocity of 76.9 mm/sec is obtained with the blowing time condition of 0.6 sec and suction time of 0.8 sec. For the result of the suction/blowing time to have the maximum velocity, there is some disagreement between the theoretical (Fig. 8(b)) and the experimental (Fig. 8(c)) results. This is because we did not consider the time to deflate/inflate the rear balloon and experimental environment in simulation study.

3.2.2 In-vitro and in-vivo tests

Since the colon has a viscoelastic characteristic, the optimized blowing/suction time is re-investigated under in-vitro condition. As an experimental result, the blowing time of 0.7 sec and suction time of 1.2 sec are required to overcome this viscoelastic characteristic.

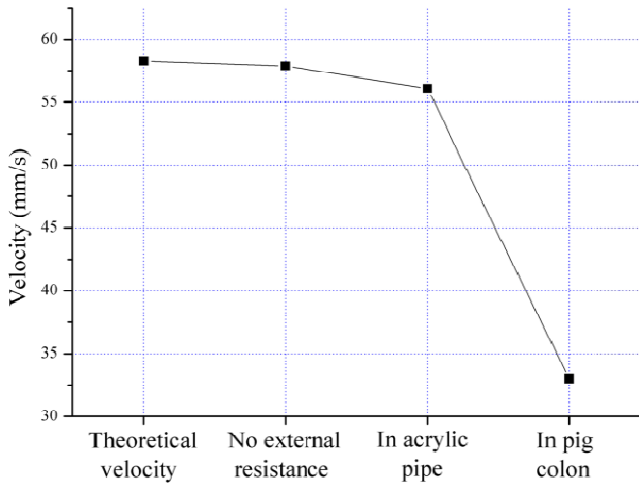

Fig. 9 Robot velocity according to experimental environment

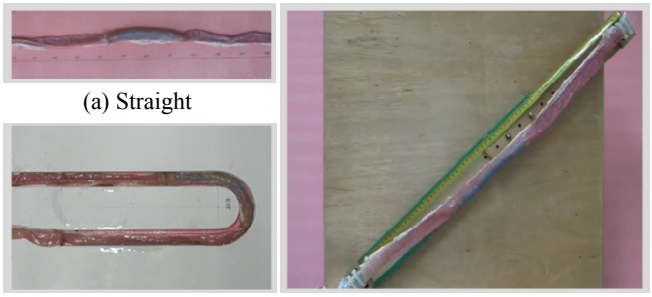

Fig. 10 Experimental environment for in-vitro test

In order to understand changes in velocity according to changes in experimental environment (Fig. 9), the theoretical velocity (bellows stroke/unit time), the velocity in the acrylic pipe and velocity under in-vitro condition are compared with the operation condition of a blowing pressure of 650 kPa and suction pressure of 17.33 kPa, as well as a blowing time of 0.7 sec and suction time of 1.2 sec. As we expected, the biggest velocity reduction occurs under in-vitro condition, and it decreases as much as 43% compared to the theoretical velocity due to the slippery and viscoelastic characteristic of the colon. The human colon consists of various configurations such as strait, curved and sloped shapes (Fig. 10). Therefore, a locomotion test is carried out in the U-shaped colon with radii of 25 mm, 30 mm, 35 mm, and 40 mm. The robot is then also evaluated in the colon with various slopes. In Fig. 11(a), the velocity decreases as the radius decreases since the bending of the bellows causes a loss of driving force. Compared to the velocity in the horizontal path, the addition of slopes causes a velocity loss of 40~60% (Fig. 11(b)). Under in-vivo condition, locomotion performance is tested at an animal laboratory at Yonsei Medical University. With the operation condition of a blowing pressure of 650 kPa and suction pressure of 17.33 kPa, as well as a blowing time of 0.7 sec and suction time of 1.2 sec, an average velocity of 8.5 mm/sec is shown in the colon of a live swine with a weight of 30 kg while it moves from the rectum to the snail-like colon (Fig. 12). Conclusively, the developed robot is able to move in a real colon environment although it loses some locomotion performance.

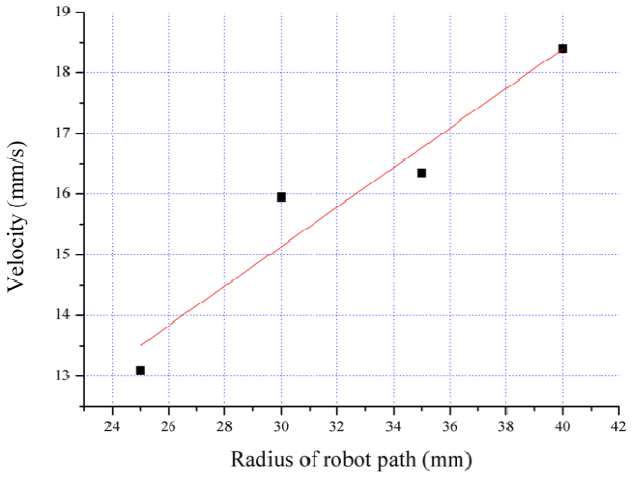

(a) According to radius of robot path

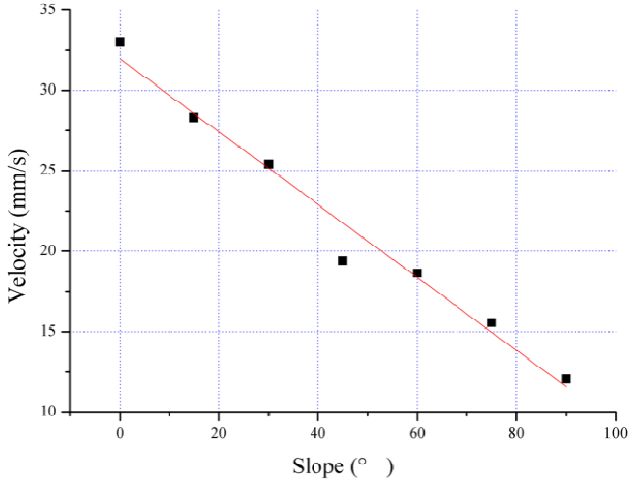

(b) According to slope of robot path

Fig. 11 Robot velocity

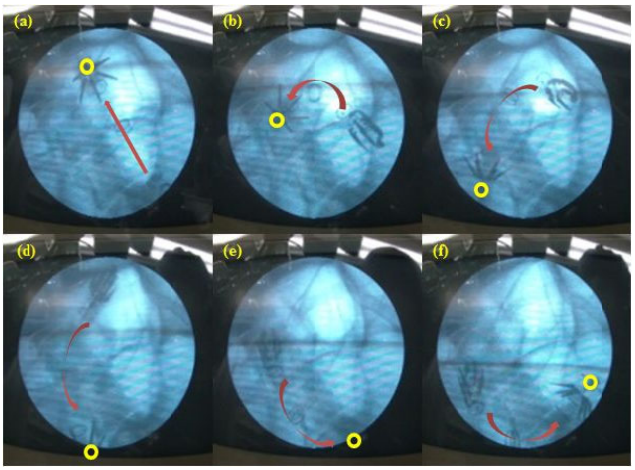

Fig. 12 Video clip for the robot (a) passing through the rectum (b) entering the snail-like colon (c)~(f) passing through the snail-like swine colon

4. Conclusion

Based on two clamping modules with 6-legs and an elongation/contraction module, an inchworm-like locomotion for

robotic colonoscope was embodied. After we fabricated the robotic colonoscope, the robot system consisting of a proportional valve, a vacuum generator and an air compressor was constructed to operate it. Next, a performance test on the robotic colonoscope system in the pipe was carried out. In particular, the velocity of the robot according to suction and insufflation time was investigated based on a theoretical analysis. This was then compared to experimental results to confirm the viability of the design.

This investigation indicated that the velocity of the robot could be satisfactorily controlled by adjusting the amount of time at which air was supplied. After we tested the locomotion performance, the robotic colonoscope was tested under in-vitro condition. Due to the viscoelastic characteristics of the colon, the velocity in a straight path of the explanted colon was 33 mm/s, a reduction value of 41% compared to that in the pipe. In the curved path, the velocity decreased as the radius of the curved course decreased since the robot was under more resistance force. In the sloped path, robot velocity varied from 33 mm/s to 12 mm/s depending on the angle of the slope path. Owing to the strong performance of the locomotive mechanism, the developed robotic colonoscope maneuvered successfully in the colon of a live swine with a speed of 8.5 mm/sec.

REFERENCES

1. Kim, K. D., Lim, H., Kim, B. K., Park, J. O., and Hong, Y. S., "A Locomotive Mechanism for Colonoscope," Transaction of the KSME, Vol. 26, No. 7, pp. 1296-1301, 2002.
2. Kim, K. D., Lee, S. J., Kim, B. K., and Park, J. O., "Radial Type Locomotive Mechanism with Worm for Robotic Endoscope," Transaction of the ICASE, Vol. 8, No. 3, pp. 220-225, 2002.
3. Kim, B. K., Lee, J. H., Lim, Y. M., Park, J. O., Kim, S. H., and Hong, Y. S., "Locomotive Colonoscope," Proceedings of the 32nd International Symposium on Robotics, pp. 1829-1833, 2001.
4. Menciassi, A., Park, J. H., Lee, S., Gorini, S., Dario, P., and Park, J. O., "Robotic Solutions and Mechanisms for a Semi-Autonomous Endoscope," Proceedings of IEEE/RSJ International Conference on Intelligent Robots and Systems, pp. 1379-1384, 2002.
5. Park, S. H., Park, H. J., Park, S. J., and Kim, B. K., "A Paddling Based Locomotive Mechanism for Capsule Endoscopes," Journal of Mechanical Science and Technology, Vol. 20, No. 7, pp. 1012-1018, 2006.
6. Kim, B. K., Lim, H. Y., Park, J. H., and Park, J. O., "Inchworm-Like Colonoscopic Robot with Hollow Body and Steering Device," JSME Int. J., Vol. 49, No. 1, pp. 205-212, 2006.
7. Lee, J. S., Kim, B. K., and Hong, Y. S., "A Flexible Chain-based Screw Propeller for Capsule Endoscopes," Int. J. Precis. Eng. Manuf., Vol. 10, No. 4, pp. 27-34, 2009.
8. Hong, Y. S., Kim, J. Y., Kwon, Y. C., and Song, S. Y., "Preliminary Study of a Twistable Thread Module on a Capsule Endoscope in a Spiral Motion," Int. J. Precis. Eng. Manuf., Vol. 12, No. 3, pp. 461-468, 2011.
9. Hoeg, H. D., Slatkin, A. B., and Burdick, J. W., "Biomechanical modeling for the small intestine as required for the design and operation of a robotic endoscope," IEEE International Conference on Robotics and Automation, pp. 1599-1606, 2000.
10. Valdastri, P., Webster, R. J., Quaglia, C., Quirini, M., Menciassi, A., and Dario, P., "A New Mechanism for Mesoscale Legged Locomotion in Compliant Tubular Environments," IEEE Transactions Robotics, Vol. 25, No. 5, pp. 1047-1057, 2009.
11. Hu, H., Wang, P., Zhao, B., Li, M., and Sun, L., "Design of a novel snake-like robotic colonoscope," Proceedings of the IEEE International Conference on Robotics and Biomimetics, pp. 1957-1961, 2009.
12. Peirs, J., Reynaerts, D., and Van Brussel, H., "Design of miniature parallel manipulators for integration in a self-propelling endoscope," Sensors and Actuators, Vol. 85, pp. 409-417, 2000.
13. Dario, P., Carroza, M. C., Lencioni, L., Magnani, B., and D'Attansio, S., "A Micro-robotics System for Colonoscopy," Proceedings of the IEEE International Conference on Robotics and Automation, pp. 1567-1572, 1997.
14. Ozaki, K., Wakimoto, S., and Suzumori, K., "Novel design of rubber tube actuator improving mountability and drivability for assisting colonosocope insertion," Proceedings of the IEEE International Conference on Robotics and Automation, pp. 3263-3268, 2011.
15. Trovato, G., Shikanai, M., Ukawa, G., Kinoshita, J., Murai, N., Lee, J. W., Ishii, H., Takanishi, A., Tanoue, K., and Ieiri, S., "Development of a colon endoscope robot that adjusts its locomotion through the use of reinforcement learning," International Journal of Computer Assisted Radiology and Surgery, Vol. 5, No. 4, pp. 317-325, 2010.
16. Phee, L., Accoto, D., Menciassi, A., Stefanini, C., Carrozza, M. C., and Dario, P., "Analysis and development of locomotion devices for the gastrointestinal tract," IEEE Transactions on Biomedical Engineering, Vol. 49, No. 6, pp. 613-616, 2002.
17. Lim, J. W., Park, H. J., An, J. M., Hong, Y. S., Kim, B. K., and Yi, B. J., "One pneumatic line based inchworm-like micro robot for half-inch pipe inspection," Mechatronics, Vol. 18, pp. 315-322, 2008.